

# Arylmagnesium to Arylcopper Conversion Monitored by Solid State Characterization of Halide Intermediates. Synthesis of Homoleptic (*o*-Vinylphenyl)copper

Henrik Eriksson, Mikael Örtendahl, and Mikael Håkansson\*

Department of Inorganic Chemistry, Chalmers University of Technology,  
S-412 96 Göteborg, Sweden

Received June 13, 1996<sup>®</sup>

The reaction between  $\text{Mg}(\text{viph})_2$  ( $\text{viph} = o\text{-vinylphenyl}$ ) and copper(I) chloride has been found to be the best way of preparing the homoleptic tetramer  $[\text{Cu}_4(\text{viph})_4]$ . The  $\text{MgR}_2$  reagent crystallizes as monomeric  $[\text{Mg}(\text{THF})_2(\text{viph})_2]$  from a THF solution. In the reaction between the Grignard reagent  $(\text{viph})\text{MgBr}$  and copper(I) chloride, two unstable mixed halide/aryl intermediates,  $[\text{Mg}(\text{THF})_6][\text{Cu}_5(\text{viph})_2\text{Br}_4]_2 \cdot \text{THF}$  (**3**) and  $[\text{Mg}(\text{THF})_5\text{Cl}][\text{Cu}_5(\text{viph})_4\text{Br}_2] \cdot \text{THF}$  (**4**), were isolated and found to reduce the yield of  $[\text{Cu}_4(\text{viph})_4]$  markedly. The crystal structures of **3** and **4** were determined and were found to exhibit unusual coordination geometries for copper(I) and provide mechanistic information. Compound **3** was found to react with excess triphenylphosphine in THF, yielding  $[\text{Cu}(\text{PPh}_3)_3\text{Br}] \cdot \text{THF}$ . It is suggested that  $[\text{Cu}_4(\text{viph})_4]$ , which is not  $\pi$ -coordinated in the solid state or in THF solution, may have important precursor qualities for the preparation of new organocopper compounds.

## Introduction

Stabilization of arylcopper complexes by nitrogen donor substituents in the *ortho* position, frequently resulting in planar tetrameric structures, has been established in a number of cases by van Koten *et al.*<sup>1</sup> We are interested in examining the effects—on stability, reactivity, and structure—of substituting unsaturated functionalities into different ring positions, thus exploiting aryl ligands that can coordinate to copper(I) simultaneously *via*  $\sigma$ - and  $\pi$ -bonds. It is well known that alkene and alkyne fragments coordinate considerably more weakly to copper(I) than do nitrogen donors, which means that labile complexes can be expected to form. In this work, we use a vinyl group in the *ortho* position to copper, which should destabilize the planar tetrameric structure relative to new  $\pi$ -coordinated structures, since the vinyl group is not sufficiently long to permit  $\pi$ -coordination to the bridging copper atoms, and thus requires a third copper center,  $\text{Cu}^*$ , as illustrated in Figure 1. We refer to the *o*-vinylphenyl ligand as “viph”.

In our search for the best synthetic route to homoleptic organocopper compounds, we chose magnesium reagents rather than lithium reagents, since we hoped this would present a way of reducing the problem of halide contamination (and coordination), by precipitation of magnesium halides as the dioxane complex. Although  $[\text{MgCu}_4\text{Ph}_6(\text{OEt}_2)]$  is structurally characterized<sup>2</sup> it appears that magnesium less easily—as compared to lithium—forms mixed organocopper aggregates. Either way, the structural aspects of magnesium organocuprates have been considerably less studied than those of the lithium diorganocuprate counterparts,

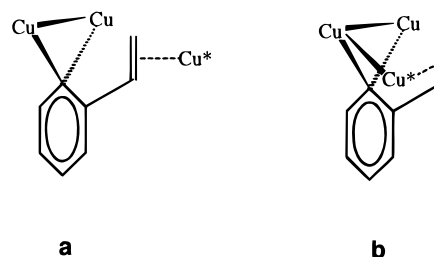


**Figure 1.** The viph ligand gives rise to a coordination polymer (a) or a cluster (b).

despite promising catalytic implications for the former. Apart from halide contamination, reductive elimination of coupling products is usually a problem encountered in arylcopper chemistry. We decided to investigate if the viph ligand would provide stabilization, with respect to aryl ligands that lack potentially coordinating substituents, and thus minimize the problem of copper reduction.

We predict that the methodology used in this work, whereby reactions are monitored by crystal structures of labile species, will become increasingly important. Further development of low-temperature techniques for isolating, crystallizing, and handling sensitive complexes and increased knowledge on how to relate solid state spectroscopic data to solution data will make the case for this methodology even stronger.

## Results and Discussion

When the Grignard reagent  $(\text{viph})\text{MgBr}$  (**1**) was added to a suspension of  $\text{CuCl}$  in THF at  $-20^\circ\text{C}$ , the copper(I) chloride dissolved quickly, yielding a bright yellow solution. We believe this to be due to the formation of a soluble magnesium halide–copper halide complex, possibly containing viph groups bonded to magnesium or else purely inorganic due to  $(\text{viph})\text{MgBr}$  transformation to  $\text{Mg}(\text{viph})_2$  (**2**) and  $\text{MgBr}_2$  according to the Schlenk equilibrium, and subsequent complexation between

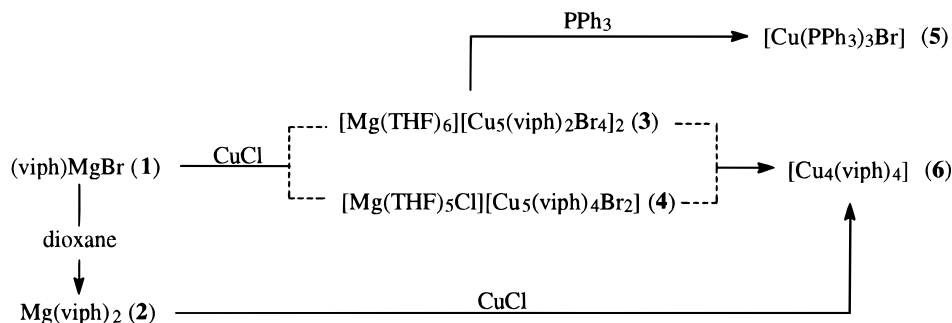
<sup>®</sup> Abstract published in *Advance ACS Abstracts*, October 1, 1996.

(1) (a) van Koten, G. *J. Organomet. Chem.* **1990**, *400*, 283. (b) van Koten, G.; James, S. L.; Jastrzebeski, J. T. B. H. *Compr. Organomet. Chem.* **1995**, *3*, 57.

(2) (a) Seitz, L. M.; Madl, R. *J. Organomet. Chem.* **1972**, *34*, 415. (b) Khan, S. I.; Edwards, P. G.; Yuan, H. S. H.; Bau, R. *J. Am. Chem. Soc.* **1985**, *107*, 1682.

**Table 1. Crystallographic Data for 2–6**

compd	2	3	4	5	6
formula	C <sub>24</sub> H <sub>30</sub> MgO <sub>2</sub>	C <sub>64</sub> H <sub>84</sub> Br <sub>8</sub> Cu <sub>10</sub> MgO <sub>7</sub>	C <sub>56</sub> H <sub>76</sub> Br <sub>2</sub> ClCu <sub>5</sub> MgO <sub>6</sub>	C <sub>58</sub> H <sub>53</sub> BrCuOP <sub>3</sub>	C <sub>32</sub> H <sub>28</sub> Cu <sub>4</sub>
fw	374.8	2264.4	1382.5	1002.4	666.8
color	white	yellow	yellow	white	white
cryst syst	monoclinic	monoclinic	monoclinic	monoclinic	triclinic
space group	<i>P</i> 2 <sub>1</sub> / <i>n</i> (No. 14)	<i>P</i> 2 <sub>1</sub> / <i>n</i> (No. 14)	<i>P</i> 2 <sub>1</sub> / <i>c</i> (No. 14)	<i>P</i> 2 <sub>1</sub> / <i>c</i> (No. 14)	<i>P</i> <i>1</i> (No. 2)
<i>a</i> , Å	9.624(2)	12.649(4)	10.276(4)	13.310(2)	9.591(1)
<i>b</i> , Å	16.448(3)	24.876(3)	23.100(6)	10.183(1)	9.693(2)
<i>c</i> , Å	14.199(4)	13.550(5)	25.530(5)	36.412(6)	8.074(4)
α, deg	90	90	90	90	110.95(2)
β, deg	105.41(2)	104.08	94.21(2)	94.86(1)	97.97(2)
γ, deg	90	90	90	90	89.90(1)
<i>V</i> , Å <sup>3</sup>	2166.7(9)	4136(4)	6044(5)	4917(2)	693.3(4)
<i>Z</i>	4	2	4	4	1
<i>d</i> <sub>calc</sub> , g/cm <sup>3</sup>	1.149	1.818	1.519	1.462	1.597
μ, cm <sup>−1</sup>	0.92	46.22	31.45	21.90	30.55
<i>T</i> , °C	−110	−120	−125	20	−110
<i>R</i>	0.071	0.062	0.069	0.058	0.054
<i>R</i> <sub>w</sub>	0.074	0.079	0.083	0.059	0.065

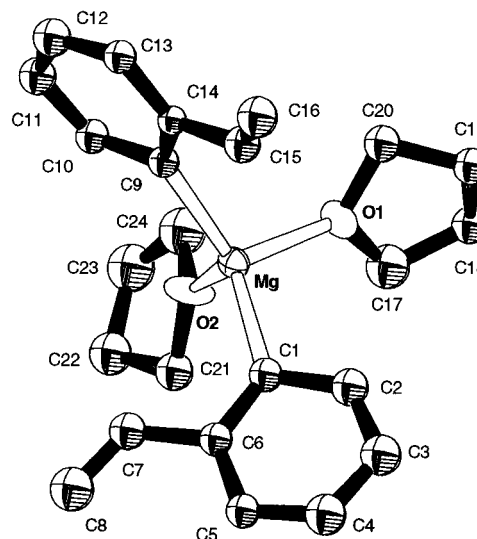
**Scheme 1**

CuCl and MgBr<sub>2</sub>. Support for this assumption, *i.e.*, that the yellow solution that forms initially does not yet contain any Cu–C  $\sigma$ -bonded species, is provided by the isolation of the two intermediates [Mg(THF)<sub>6</sub>][Cu<sub>5</sub>(viph)<sub>2</sub>Br<sub>4</sub>]<sub>2</sub>·THF (3), which crystallized only after dioxane addition and several hours at 0 °C, and [Mg(THF)<sub>5</sub>Cl][Cu<sub>5</sub>(viph)<sub>4</sub>Br<sub>2</sub>]<sub>2</sub>·THF (4), which crystallized from a different solution only after an extended reaction time of several days at −20 °C. Compound 3 was dissolved in THF by the addition of triphenylphosphine, resulting in a solution from which [Cu(PPh<sub>3</sub>)<sub>3</sub>Br]·THF (5) was crystallized in approximately 50% yield. From the remaining solution it was not possible to isolate any further copper complex.

In order to exclude the formation of bromide-bridged intermediates, we decided to react the halide-free Mg(viph)<sub>2</sub> reagent with copper(I) chloride, which resulted in the homoleptic copper aryl, [Cu<sub>4</sub>(viph)<sub>4</sub>] (6). The yield was, however, somewhat reduced (65%) by the decreased solubility of CuCl in the bromide-free solution.

Evaporation to dryness, under reduced pressure, of the solutions from which 3 and 4 crystallized, and subsequent extraction with toluene, also gave 6, but in very low yield (typically <5%). Attempts to dissolve solid 3 and 4 in THF in order to produce 6 were unsuccessful on account of the low solubility and high sensitivity of 3 and 4. The different reactions and complexes are summarized in Scheme 1.

**Structure of [Mg(THF)<sub>2</sub>(viph)<sub>2</sub>] (2).** As can be seen from Figure 2, 2 crystallizes as a monomer, in which magnesium is coordinated by two THF molecules and two viph ligands. The magnesium atom is approximately tetrahedrally coordinated, with the O(1)–Mg–O(2) bond angle being significantly more acute (91.2°) than the corresponding C(1)–Mg–C(2) bond

**Figure 2.** Crystallographic numbering in [Mg(THF)<sub>2</sub>(viph)<sub>2</sub>] (2).

angle (127.8°), a situation that appears to be common in organomagnesium chemistry,<sup>3</sup> and several arylmagnesium species have been structurally characterized.<sup>4</sup> There are no interactions between the  $\pi$  electrons of the vinyl groups and magnesium. The Mg–C and Mg–O bond distances are normal. Positional and thermal parameters are listed in the Supporting Information, and relevant bond distances and angles are presented in Table 2. The shortest intermolecular H···H distances are approximately 2.7 Å.

(3) Markies, P. R.; Ackerman, O. S.; Bickelhaupt, F.; Smeets, W. J. J.; Spek, A. L. *Adv. Organomet. Chem.* **1991**, 32, 147.

(4) Bickelhaupt, F. *J. Organomet. Chem.* **1994**, 475, 1.

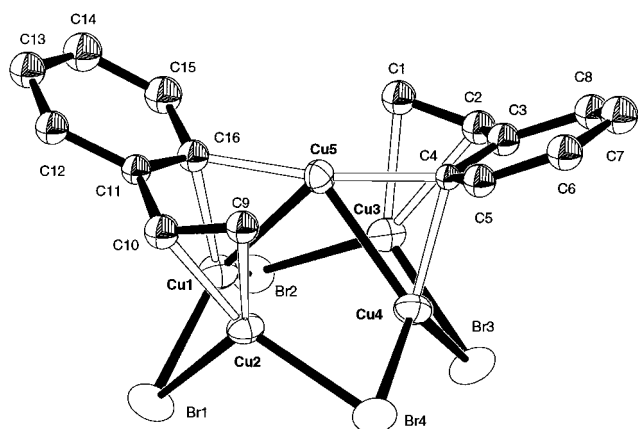


**Figure 3.** Crystallographic numbering in  $[\text{Cu}_5(\text{viph})_2\text{Br}_4]^-$ , the anion of **3**. The  $\text{Cu}\cdots\text{Cu}$  interactions, which are shorter than 2.5 Å, are indicated with tapered black "bonds". Both vinyl groups coordinate to copper, forming a trigonal coordination plane with two bromides, respectively.

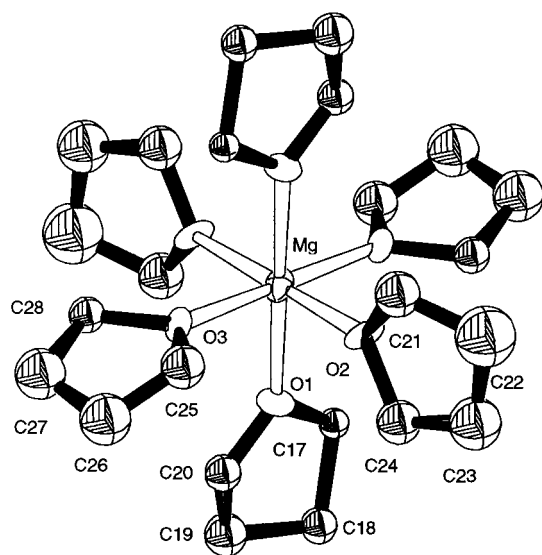


**Figure 4.** Crystallographic numbering in  $[\text{Mg}(\text{THF})_6]^{2+}$ , the cation of **3**.

**Table 2. Selected Intramolecular Distances (Å) and Angles (Deg) for  $[\text{Mg}(\text{THF})_2(\text{viph})_2]^{2+}$  (2)**

Mg—O(1)	2.044(8)	C(1)—C(2)	1.42(1)
Mg—O(2)	2.027(8)	C(2)—C(3)	1.38(1)
Mg—C(1)	2.14(1)	C(3)—C(4)	1.34(1)
Mg—C(2)	2.14(1)	C(4)—C(5)	1.38(2)
O(1)—C(17)	1.44(1)	C(5)—C(6)	1.40(1)
O(1)—C(20)	1.43(1)	C(7)—C(8)	1.30(2)
O(2)—C(21)	1.44(1)	C(14)—C(15)	1.50(2)
O(2)—C(24)	1.45(1)	C(15)—C(16)	1.32(2)
O(1)—Mg—O(2)	91.2(4)	C(6)—C(1)—C(2)	113(1)
O(1)—Mg—C(1)	107.4(4)	C(14)—C(9)—C(10)	113(1)
O(1)—Mg—C(9)	109.5(4)	C(6)—C(7)—C(8)	127(1)
O(2)—Mg—C(1)	109.8(4)	C(14)—C(15)—C(16)	127(1)
O(2)—Mg—C(9)	105.1(4)	C(17)—O(1)—C(20)	107.0(9)

**Structure of  $[\text{Mg}(\text{THF})_6][\text{Cu}_5(\text{viph})_2\text{Br}_4] \cdot \text{THF}$  (**3**).** The anionic cluster  $[\text{Cu}_5(\text{viph})_2\text{Br}_4]^-$  is depicted in Figure 3, while the  $[\text{Mg}(\text{THF})_6]^{2+}$  cation is shown in Figure 4. Positional and thermal parameters are listed in the Supporting Information, and selected bond distances and angles are given in Table 3. The anion features a square pyramidal copper core, in which the four basal copper atoms are bridged by four bromide atoms, thus forming an eight-membered ring, resem-

**Table 3. Selected Intramolecular Distances (Å) and Angles (Deg) for  $[\text{Mg}(\text{THF})_6][\text{Cu}_5(\text{viph})_2\text{Br}_4] \cdot \text{THF}$  (**3**)**

Br(1)—Cu(1)	2.416(7)	Br(1)—Cu(2)	2.414(7)
Br(2)—Cu(1)	2.392(7)	Br(2)—Cu(3)	2.370(7)
Br(3)—Cu(3)	2.392(7)	Br(3)—Cu(4)	2.420(7)
Br(4)—Cu(2)	2.393(7)	Br(4)—Cu(4)	2.389(7)
Cu(1)—Cu(2)	2.709(7)	Cu(1)—Cu(3)	2.919(7)
Cu(1)—Cu(4)	3.228(6)	Cu(1)—Cu(5)	2.467(7)
Cu(2)—Cu(4)	2.926(7)	Cu(2)—Cu(5)	2.846(7)
Cu(3)—Cu(4)	2.690(7)	Cu(3)—Cu(5)	2.889(7)
Cu(4)—Cu(5)	2.458(7)	Cu(1)—C(16)	2.12(4)
Cu(5)—C(16)	1.98(4)	Cu(2)—C(9)	2.08(4)
Cu(2)—C(10)	2.12(4)	Cu(4)—C(4)	2.10(4)
Cu(5)—C(4)	1.95(4)	Cu(3)—C(1)	2.04(4)
Cu(3)—C(2)	2.17(4)	C(1)—C(2)	1.31(5)
C(2)—C(3)	1.58(5)	C(3)—C(4)	1.43(4)
C(4)—C(5)	1.40(5)	C(5)—C(6)	1.41(5)
C(6)—C(7)	1.41(5)	C(7)—C(8)	1.40(5)
C(9)—C(10)	1.33(4)	C(10)—C(11)	1.49(5)
Cu(5)—H(1B)	2.56	Mg—O(1)	2.08(2)
Mg—O(2)	2.06(2)	Mg—O(3)	2.02(2)
O(1)—C(17)	1.50(4)	O(1)—C(20)	1.32(4)
O(2)—C(21)	1.39(5)	O(2)—C(24)	1.38(5)
O(3)—C(25)	1.45(4)	O(3)—C(28)	1.47(4)
Cu(1)—Br(1)—Cu(2)	68.2(2)	Cu(1)—Br(2)—Cu(3)	75.6(2)
Cu(3)—Br(3)—Cu(4)	68.0(2)	Cu(2)—Br(4)—Cu(4)	75.4(2)
Br(1)—Cu(1)—Br(2)	118.0(3)	Br(1)—Cu(2)—Br(4)	107.9(3)
Br(2)—Cu(3)—Br(3)	109.7(3)	Br(3)—Cu(4)—Br(4)	116.8(3)
Cu(1)—Cu(5)—Cu(4)	81.9(2)	Cu(2)—Cu(1)—Cu(5)	66.5(2)
Cu(1)—C(16)—Cu(5)	74(1)	Cu(4)—C(4)—Cu(5)	75(1)
C(1)—C(2)—C(3)	119(4)	C(9)—C(10)—C(11)	128(3)
O(1)—Mg—O(2)	90(1)	O(1)—Mg—O(3)	89(1)
O(2)—Mg—O(3)	91.6(9)	Mg—O(1)—C(17)	125(2)

bling the coordination found in the  $[\text{Cu}_6\text{Br}_9]^{3-}$  anion;<sup>5</sup> Cu—Br bond distances are also in the same range as in previously known bromocuprates.<sup>6</sup> Previously known mixed aryl/halide copper(I) complexes are neutral aggregates where the number of copper atoms is three as in  $[\text{Cu}_3\{\text{C}_6\text{H}_4\text{CH}_2\text{N}(\text{Me})\text{CH}_2\text{NMe}_2\cdot 2\}_2\text{Br}_2]$ ,<sup>7a</sup> four as in  $[\text{Cu}_4(\text{C}_6\text{H}_3(\text{CH}_2\text{NMe}_2)_2\cdot 2,6)_2\text{Br}_2]$ <sup>7b</sup> and  $[\text{Cu}_4(\text{C}_{18}\text{H}_{20}\text{N})_2\cdot 2\text{Br}_2]$ ,<sup>7c</sup> five as in  $[\text{Cu}_5\{\text{C}_6\text{H}_3(\text{CH}_2\text{N}(\text{Me})\text{CH}_2\text{CH}_2\text{NMe}_2)_2\cdot 2,6\}_2\text{Br}_3]$ ,<sup>7d</sup> or six as in  $[\text{Cu}_6(\text{C}_6\text{H}_4\text{NMe}_2)_4\text{Br}_2]$ <sup>7e</sup> and  $[\text{Cu}_6(\text{MeOXL}_4)\text{Br}_2]$ .<sup>7f</sup> Compounds **3** and **4** appear, however, to exhibit the first examples of anionic mixed aryl/halide copper species. The bromide/copper ratio of 4:5 in **3** is unusually high as compared to the above-mentioned neutral complexes where the ratio in no case exceeds 1:2. The apical copper atom in **3**, Cu(5), is bridged, *via*  $2e^-$ – $3c$ -bonds of the viph ligands, to two of the basal copper atoms, Cu(1) and Cu(4), while the other two, Cu(2) and Cu(3), are  $\pi$ -coordinated to the vinyl groups of the viph ligands. The Cu(1)–aryl–Cu(5)–aryl–C(4) fragment has become a well-known motif in arylcopper chemistry, which can be seen, *e.g.*, in pentameric mesitylcopper<sup>8</sup> or in tetrameric (2,4,6-triisopro-

(5) Andersson, S.; Jagner, S. *Acta Chem. Scand.* **1989**, 43, 39.

(6) Jagner, S.; Helgesson, G. *Adv. Inorg. Chem.* **1991**, 37, 1.

(7) (a) Janssen, M. D.; Grove, D. M.; Spek, A. L.; van Koten, G. *XVth International Conference on Organometallic Chemistry*; Royal Society of Chemistry: London, 1994; Book of Abstracts, OC.9. (b) Wehman, E.; van Koten, G.; Erkamp, J. M.; Knottner, D. M.; Jastrzebski, J. T. B. H.; Stam, C. H. *Organometallics* **1989**, 8, 94. (c) Smeets, W. J. J.; Spek, A. L. *Acta Crystallogr. C* **1987**, 43, 870. (d) Kapteijn, G. M.; Wehman-Ooyevaar, I. C. M.; Grove, D. M.; Smeets, W. J. J.; Spek, A. L.; van Koten, G. *Angew. Chem., Int. Ed. Engl.* **1993**, 32, 72. (e) Guss, J. M.; Mason, R.; Thomas, K. M.; van Koten, G.; Noltes, J. G. *J. Organomet. Chem.* **1972**, 40, C79. (f) Wehman, E.; van Koten, G.; Jastrzebski, J. T. B. H.; Rotteveel, M. A.; Stam, C. H. *Organometallics* **1988**, 7, 1477.

(8) Gambarotta, S.; Floriani, C.; Chiesi-Villa, A.; Guastini, C. *J. Chem. Soc., Chem. Commun.* **1983**, 1156.

pylphenyl)copper.<sup>9</sup> The copper–copper distances in  $[\text{Cu}_5(\text{viph})_2\text{Br}_4]^-$  are in good agreement with those previously determined for arylbridged copper clusters. The midpoint of the double bond between C(9) and C(10), *cf.* Figure 3, are together with Br(1) and Br(4) trigonally coordinated to Cu(2). The double bond is approximately parallel to this trigonal plane, which is indicative of three-coordinated copper.<sup>10a</sup> The analogous reasoning applies of course to the coordination around Cu(3). Within the precision of the crystallographic data, it is not possible to detect any lengthening of the vinyl C=C double bonds on coordination to copper. A weak interaction is thus indicated, which is in accordance with earlier results.<sup>10</sup> It should, however, be pointed out that simultaneous  $\sigma$ -carbon and C=C  $\pi$ -coordination is a rare phenomenon in organocopper complexes, in spite of the fact that  $\pi$ -coordination to copper is believed to be the initial reaction step in the conjugate addition of organocuprate reagents to enone substrates.<sup>1b</sup> Figure 3 indicates how small alterations in the geometry of this type of complexes could result in an ideal situation for agostic interactions around Cu(5). In the present molecule, however, the Cu(5)···H(1B) distance is approximately 2.56 Å, which is too long for any appreciable interaction. The octahedrally coordinated (*cf.* Figure 4) magnesium cation,  $[\text{Mg}(\text{THF})_6]^{2+}$ , displays a mean Mg–O bond distance of 2.05 Å, which is somewhat shorter than that found in  $[\text{Mg}(\text{THF})_6][\text{MoOCl}_4(\text{THF})_2]_2$ , where a distortion of the octahedron in terms of two longer Mg–O bonds (2.156 Å) and four shorter Mg–O bonds (the mean value is 2.092 Å) was reported.<sup>9</sup> No such distortion (within the precision of our data) is observed in the present cation.

**Structure of  $[\text{Mg}(\text{THF})_5\text{Cl}][\text{Cu}_5(\text{viph})_4\text{Br}_2]\cdot\text{THF}$  (4).** The anionic cluster  $[\text{Cu}_5(\text{viph})_4\text{Br}_2]^-$  is depicted in Figure 5, while the cation  $[\text{Mg}(\text{THF})_5\text{Cl}]^+$  is shown in Figure 6. Positional and thermal parameters are listed in the Supporting Information, and selected bond distances and angles are given in Table 4. Four of the copper atoms in  $[\text{Cu}_5(\text{viph})_4\text{Br}_2]^-$ , *viz.* Cu(1), Cu(2), Cu(3), and Cu(4), form a square planar aryl-bridged structure, resembling that in the neutral (2,4,6-triisopropylphenyl)copper,<sup>9</sup> but in the present anion the fourth bridge, that between Cu(3) and Cu(4), is afforded *via*  $\pi$ -coordination of the vinyl group to Cu(3) and not solely via the *C*<sub>ipso</sub> atom, C(25). Instead, C(25) bridges Cu(4) and Cu(5), so that the Cu(1)–Cu(4)–Cu(5) angle is 85.7°, while the Cu(3)–Cu(4)–Cu(5) angle is 67.3°. In addition, Cu(3) and Cu(4) are connected via a bridging bromide, Br(2), while Cu(5) is bonded to a terminal bromide, Br(1). This existence of a terminally bonded bromide is unique, since all previously known mixed aryl/halide copper complexes feature bromides bridging two or three copper atoms. The Br/Cu ratio of 2:5 is well in the range found for neutral mixed aryl/halide copper complexes, but **4** is structurally more related to tetrameric species like  $[\text{Cu}_4(\text{C}_6\text{H}_3(\text{CH}_2\text{NMe}_2)_2-2,6)_2\text{Br}_2]^{7b}$  than to the only other known (apart from **3**) pentameric mixed aryl/halide copper complex, *viz.*

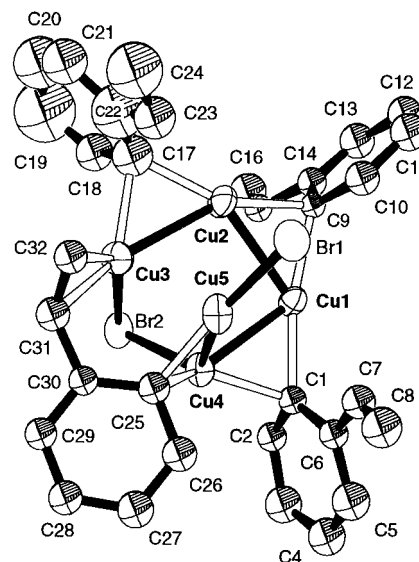


**Figure 5.** Crystallographic numbering in  $[\text{Cu}_5(\text{viph})_4\text{Br}_2]^-$ , the anion of **4**. The Cu···Cu interactions, which are shorter than 2.5 Å, are indicated with tapered black "bonds". Unusual coordination features include simultaneous  $\sigma$ - and  $\pi$ -coordination to carbon, as displayed by Cu(3), and a terminally bound bromide, *viz.* Br(1).

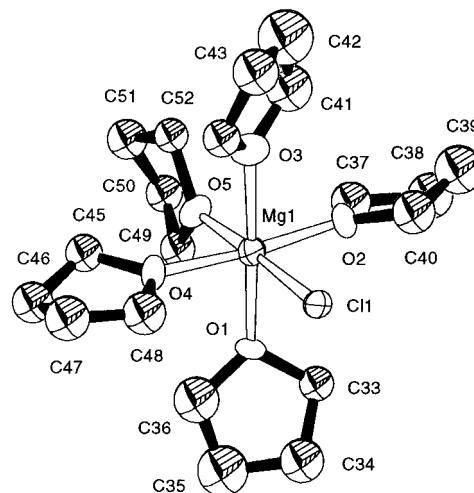


**Figure 6.** Crystallographic numbering in  $[\text{Mg}(\text{THF})_5\text{Cl}]^+$ , the cation of **4**.

$[\text{Cu}_5\{\text{C}_6\text{H}_3(\text{CH}_2\text{N}(\text{Me})\text{CH}_2\text{CH}_2\text{NMe}_2)_2-2,6\}_2\text{Br}_3]^{7d}$  which forms a substantially more expanded Cu–Br core. The coordination around Cu(3) as well as Cu(5) is highly unusual. Cu(3) exhibits a coordination that perhaps best is described as, taking the view that the Cu(2)···Cu(3) interaction is nonbonding, distorted planar trigonal. On the other hand, if the copper–copper interaction is included, the coordination can instead be described as strongly distorted tetrahedral, Cu(3) being bonded to a bridging bromide, a C=C double bond, a bridging carbon, and a copper center. The same ambiguity exists for Cu(5), but here the choice is between distorted linear coordination—the Br(1)–Cu(5)–C(25) bond angle is 165.9°—and an even more distorted trigonal planar coordination, including the Cu(5)···Cu(4) interaction. The copper–copper distances in  $[\text{Cu}_5(\text{viph})_4\text{Br}_2]^-$  are in accordance with those previously determined for aryl-bridged copper clusters. The angle between the plane of the four copper atoms (Cu(1), Cu(2), Cu(3), and Cu(4)) and the aryl ring containing C(1) is 103°, while the

(9) Nobel, D.; van Koten, G.; Spek, A. L. *Angew. Chem., Int. Ed. Engl.* **1989**, *28*, 208.

(10) (a) Håkansson, M.; Jägers, S.; Walther, D. *Organometallics* **1991**, *10*, 1317. (b) Håkansson, M.; Wettström, K.; Jägers, S. *J. Organomet. Chem.* **1991**, *421*, 347. (c) Håkansson, M.; Jägers, S.; Clot, E.; Eisenstein, O. *Inorg. Chem.* **1992**, *31*, 5389.

(11) Sobota, P.; Plucinski, T.; Lis, T. *Z. Anorg. Allg. Chem.* **1986**, *533*, 215.

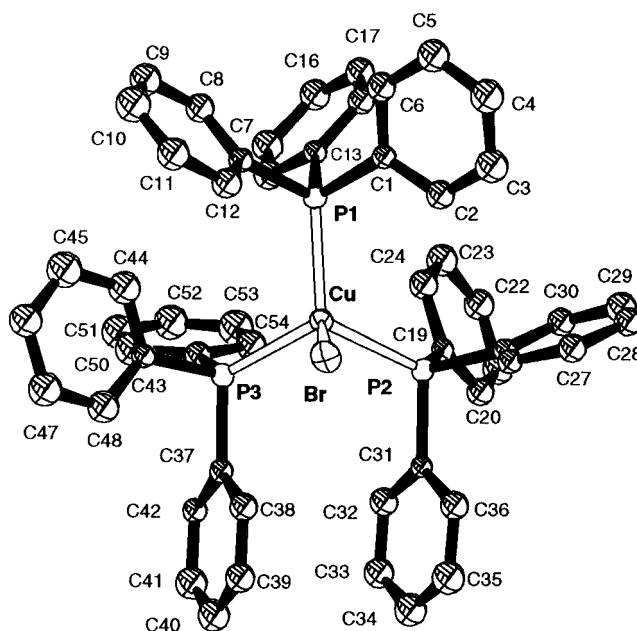
**Table 4. Selected Intramolecular Distances (Å) and Angles (Deg) for [Mg(THF)<sub>5</sub>Cl][Cu<sub>5</sub>(viph)<sub>4</sub>Br<sub>2</sub>]·THF (4)**

Br(1)–Cu(5)	2.267(4)	Br(2)–Cu(3)	2.448(4)
Br(2)–Cu(4)	2.439(4)	Cu(1)–Cu(2)	2.484(4)
Cu(1)–Cu(4)	2.441(4)	Cu(2)–Cu(3)	2.496(5)
Cu(3)–Cu(4)	2.795(5)	Cu(4)–Cu(5)	2.459(5)
Cu(1)–C(1)	1.95(2)	Cu(1)–C(9)	1.98(2)
Cu(2)–C(9)	2.02(2)	Cu(2)–C(17)	2.05(3)
Cu(3)–C(31)	2.17(3)	Cu(1)–C(32)	2.16(2)
Cu(4)–C(1)	2.09(2)	Cu(4)–C(25)	2.10(2)
Cu(5)–C(25)	1.98(2)	C(1)–C(2)	1.38(3)
C(2)–C(3)	1.38(3)	C(3)–C(4)	1.44(3)
C(4)–C(5)	1.38(3)	C(5)–C(6)	1.40(3)
C(6)–C(7)	1.41(3)	C(7)–C(8)	1.32(3)
C(25)–C(26)	1.43(3)	C(26)–C(27)	1.42(3)
C(27)–C(28)	1.43(3)	C(28)–C(29)	1.39(3)
C(29)–C(30)	1.36(3)	C(30)–C(31)	1.45(3)
C(31)–C(32)	1.34(3)	Mg(1)–Cl(1)	2.45(1)
Mg(1)–O(1)	2.11(2)	Mg(1)–O(2)	2.11(2)
Mg(1)–O(3)	2.11(2)	Mg(1)–O(4)	2.15(2)
Mg(1)–O(5)	2.14(2)	O(1)–C(33)	1.43(3)
O(1)–C(36)	1.42(3)	O(1)–C(20)	1.32(4)
O(3)–C(41)	1.47(3)	O(3)–C(44)	1.45(3)
O(5)–C(49)	1.46(3)	O(5)–C(52)	1.47(3)

Cu(3)–Br(2)–Cu(4)	69.8(1)	Br(2)–Cu(3)–Cu(2)	91.6(1)
Br(2)–Cu(4)–Cu(1)	97.1(1)	Br(1)–Cu(5)–Cu(4)	136.5(2)
Cu(1)–Cu(2)–Cu(3)	100.2(2)	Cu(2)–Cu(3)–Cu(4)	79.3(1)
Cu(1)–Cu(4)–Cu(5)	85.7(1)	Cu(3)–Cu(4)–Cu(5)	67.3(1)
Br(1)–Cu(5)–C(25)	165.9(8)	C(1)–Cu(1)–C(9)	164.8(9)
Cu(1)–C(1)–Cu(4)	74.2(8)	Cu(4)–C(25)–Cu(5)	74.2(8)
C(6)–C(7)–C(8)	131(3)	C(30)–C(31)–C(32)	129(3)
Cl(1)–Mg(1)–O(1)	90.4(5)	Cl(1)–Mg(1)–O(2)	92.8(5)
Cl(1)–Mg(1)–O(3)	93.5(5)	Cl(1)–Mg(1)–O(4)	92.9(5)
Cl(1)–Mg(1)–O(5)	175.6(6)	O(1)–Mg(1)–O(2)	90.5(7)
O(1)–Mg(1)–O(3)	176.0(7)	O(1)–Mg(1)–O(4)	91.6(6)
O(1)–Mg(1)–O(5)	85.1(6)	Mg(1)–O(1)–C(33)	121(1)

other two aryl rings (containing C(9) and C(17), respectively) are almost at right angles (94°) to the copper plane. The C(1) atom also shows the largest asymmetry with respect to the distance to the copper atoms that it bridges: the Cu(1)–C(1) bond distance is 1.95(2) Å, while the Cu(4)–C(1) bond distance is 2.09(2) Å. An interesting feature is the fact that C(1), C(9), and C(17) all are displaced in the same direction, i.e., opposite to Cu(5), with respect to the plane through the four copper atoms, the displacement being 0.09, 0.15, and 0.29 Å, respectively. Within the precision of the crystallographic data, it is not possible to see any lengthening of the vinyl C(31)–C(32) double bond—it is 1.34(3) Å—on coordination to copper, indicating a weak interaction. The Cu–Br distances for the terminal Br(1) and the bridging Br(2) are normal. The [Mg(THF)<sub>5</sub>Cl]<sup>+</sup> cation is a rare species, and even though it has been predicted to exist in solutions containing Grignard reagents,<sup>12</sup> this is, to our knowledge, the first example of the crystallization of [Mg(THF)<sub>5</sub>Cl]<sup>+</sup> from such solutions. The cation has, however, recently been synthesized and structurally characterized as [Mg(THF)<sub>5</sub>Cl][FeCl<sub>4</sub>]·THF and [Mg(THF)<sub>5</sub>Cl][AlCl<sub>4</sub>]·THF.<sup>12</sup> The Mg–Cl bond distance in the present cation is 2.45(1) Å, which is somewhat longer than in the previously studied cations (2.39(1) Å).<sup>10</sup> The Mg–O bond distances are, however, not significantly different. Discussion concerning the distortion of the octahedral coordination figure is not meaningful, owing to the precision of the present structural results.

**Structure of [Cu(PPh<sub>3</sub>)<sub>3</sub>Br]·THF (5).** As expected, triphenylphosphine readily displaces the viph ligands,

**Figure 7.** Crystallographic numbering in [Cu(PPh<sub>3</sub>)<sub>3</sub>Br] (5). The molecule displays only approximate C<sub>3</sub> symmetry along the Cu–Br bond.**Table 5. Selected Intramolecular Distances (Å) and Angles (Deg) for [Cu(PPh<sub>3</sub>)<sub>3</sub>Br]·THF (5)**

Cu–P(1)	2.351(3)	Cu–P(2)	2.352(3)
Cu–P(3)	2.340(3)	Cu–Br	2.439(2)
P(1)–C(1)	1.813(9)	P(1)–C(7)	1.83(1)
P(1)–C(13)	1.82(1)	P(2)–C(19)	1.820(9)
P(2)–C(25)	1.842(9)	P(2)–C(31)	1.838(9)
P(3)–C(37)	1.81(1)	P(3)–C(43)	1.85(1)
P(3)–C(49)	1.83(1)	C(1)–C(2)	1.37(1)
Br–Cu–P(1)	102.51(8)	Br–Cu–P(2)	101.60(8)
Br–Cu–P(3)	102.51(8)	P(1)–Cu–P(2)	118.5(1)
P(1)–Cu–P(3)	115.7(1)	P(2)–Cu–P(3)	112.0(1)

yielding **5**. [Cu(PPh<sub>3</sub>)<sub>3</sub>Br]·THF, which is shown in Figure 7, differs from the previously known phases of Cu(PPh<sub>3</sub>)<sub>3</sub>Br in that one molecule of the THF solvent is cocrystallized. In [Cu(PPh<sub>3</sub>)<sub>3</sub>Br]<sup>13</sup> as well as in the chloro analogue of (5), [Cu(PPh<sub>3</sub>)<sub>3</sub>Cl]·3THF,<sup>14</sup> there is a crystallographic 3-fold axis along the M–X bond. Such crystallographic C<sub>3</sub> symmetry is not present in **5** or in [Cu(PPh<sub>3</sub>)<sub>3</sub>Br]·2CH<sub>3</sub>CO,<sup>13</sup> but the molecules can, of course, be described as having approximate C<sub>3</sub> symmetry. The mean Cu–P bond distance of 2.344(3) Å and the Cu–Br bond distance of 2.439(2) Å, in the present molecule, does not differ significantly from those determined previously,<sup>13,14</sup> but the precision in the present determination is higher. Positional parameters and relevant bond distances and angles are given in the Supporting Information and Table 5.

**Structure of [Cu<sub>4</sub>(viph)<sub>4</sub>] (6).** Homoleptic arylcopper compounds that exclusively exhibit carbon atoms bonded to copper are scarce. While mesitylcopper obtained from toluene has been shown to be pentameric in the solid state, the copper atoms forming an approximately planar five-membered ring,<sup>8</sup> the tetrameric (2,4,6-triisopropylphenyl)copper<sup>9</sup> exhibits copper atoms forming a square planar arrangement, an arrangement

(13) Barron, P. F.; Dyason, J. C.; Healy, P. C.; Engelhardt, L. M.; Pakawatchai, C.; Patrick, V. A.; White, A. H. *J. Chem. Soc., Dalton Trans.* **1987**, 1099.

(14) Folting, K.; Huffman, J.; Mahoney, W.; Stryker, J. M.; Caulton, K. G. *Acta Crystallogr.* **1987**, C43, 1490.

(12) Sobota, P.; Plucinski, T.; Utko, J.; Lis, T. *Inorg. Chem.* **1989**, 28, 2217.

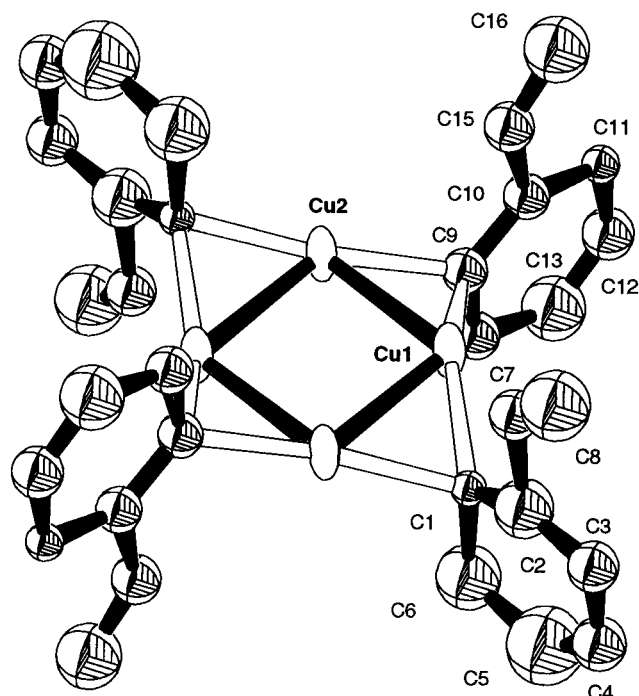


**Figure 8.** Crystallographic numbering in  $[\text{Cu}_4(\text{viph})_4]$  (**6**), exhibiting an approximately square planar tetramer, while none of the vinyl groups coordinates to copper. The  $\text{Cu}\cdots\text{Cu}$  interactions, which are shorter than 2.5 Å, are indicated with tapered black "bonds".

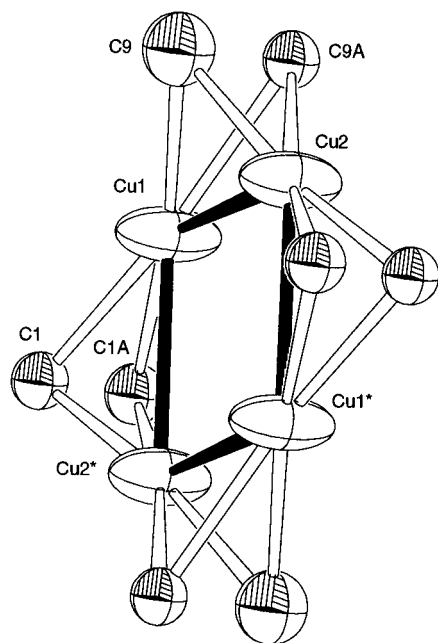


**Figure 9.** The  $\text{C}_{\text{ipso}}$  atoms in **6** are disordered and displaced approximately 0.6 Å away from the copper plane.

also found in **6**; see Figures 8 and 9. Not only is this square planar structure frequently found in arylcopper complexes stabilized with heteroatoms in the *ortho*-position<sup>1</sup> but also in nonaryl complexes such as  $[\text{Cu}_4(\text{CH}_2\text{-TMS})_4]$ <sup>15</sup> or  $[\text{Cu}_4(\text{O}-t\text{-Bu})_4]$ .<sup>16</sup> There is serious disorder associated with **6**, to the effect that the molecule becomes crystallographically centrosymmetric. In Figure 8, only four of the  $\text{C}_{\text{ipso}}$  carbons, which all have 0.5

**Table 6.** Selected Intramolecular Distances (Å) and Angles (Deg) for  $[\text{Cu}_4(\text{viph})_4]$  (**6**)

$\text{Cu}(1)-\text{Cu}(2)$	2.406(2)	$\text{Cu}(1)-\text{Cu}(2)^*$	2.401(2)
$\text{Cu}(1)-\text{C}(1)$	2.02(2)	$\text{Cu}(1)-\text{C}(9)$	1.98(2)
$\text{Cu}(2)-\text{C}(9)$	2.01(2)	$\text{Cu}(2)^*-\text{C}(1)$	2.01(2)
$\text{C}(1)-\text{C}(2)$	1.18(2)	$\text{C}(2)-\text{C}(3)$	1.38(2)
$\text{C}(3)-\text{C}(4)$	1.38(3)	$\text{C}(4)-\text{C}(5)$	1.43(3)
$\text{C}(5)-\text{C}(6)$	1.55(4)	$\text{C}(2)-\text{C}(7)$	1.62(3)
$\text{C}(7)-\text{C}(8)$	1.25(3)	$\text{C}(9)-\text{C}(10)$	1.29(2)
$\text{C}(10)-\text{C}(11)$	1.36(2)	$\text{C}(11)-\text{C}(12)$	1.47(3)
$\text{C}(12)-\text{C}(13)$	1.24(3)	$\text{C}(13)-\text{C}(14)$	1.51(3)
$\text{C}(10)-\text{C}(15)$	1.66(3)	$\text{C}(15)-\text{C}(16)$	1.25(3)
$\text{Cu}(2)-\text{Cu}(1)-\text{Cu}(2)^*$	90.56(6)	$\text{C}(1)-\text{Cu}(1)-\text{C}(9)$	145(1)
$\text{C}(1)-\text{Cu}(1)-\text{C}(9\text{A})$	166.4(7)	$\text{Cu}(1)-\text{C}(9)-\text{Cu}(2)$	74.1(7)
$\text{Cu}(1)-\text{C}(9\text{A})-\text{Cu}(2)$	71.3(6)	$\text{Cu}(1)-\text{C}(1)-\text{Cu}(2)^*$	73.2(6)
$\text{Cu}(1)-\text{C}(1\text{A})-\text{Cu}(2)^*$	73.7(6)	$\text{C}(2)-\text{C}(7)-\text{C}(8)$	128(2)

atom site occupancy, are displayed together with the other carbons that complete the respective viph ligands. In Figure 8, the center of symmetry has been retained, so that the two vinyl groups on the same side of the plane of the four copper atoms are positioned in a *trans* configuration. The *cis* configuration without a center of symmetry is, of course, equally probable. In Figure 9, all eight  $\text{C}_{\text{ipso}}$  carbons are displayed, while the other carbon atoms have been omitted for clarity. It is likely that this solid state disorder results from molecules exhibiting a geometry much like that found in (2,4,6-triisopropylphenyl)copper,<sup>9</sup> with different orientations in different unit cells. This is supported by the magnitudes of the displacements of the  $\text{C}_{\text{ipso}}$  carbons from the copper plane. In (2,4,6-triisopropylphenyl)copper the  $\text{C}_{\text{ipso}}$  carbons are displaced approximately 0.58 Å from the mean copper plane, and in **6** these distances are in the range of 0.52–0.63 Å. Unfortunately, detailed discussion of the geometrical arrangement of the aryl ligands in **6** is precluded, on account of the severe disorder. The copper–copper interactions are of the same magnitude as previously observed in (triisopropylphenyl)copper.<sup>9</sup> Positional and thermal parameters are listed in the Supporting Information. Relevant bond distances and angles are given in Table 6.

Synthetic routes to pure organocopper compounds have been the object of extensive investigation.<sup>1b</sup> Organolithium, organomagnesium, or organozinc reagents are usually employed in a metathesis reaction with a copper halide, and a frequent problem is that of halide complexation of the intended organocopper product. In addition to the choice of the organometallic reagent, also frequently the nature of the copper(I) halide, the stoichiometry and the order of addition are vital. Our results show that for the synthesis of homoleptic  $\text{Cu}_4(\text{viph})_4$ , a convenient method is to use the  $\text{Mg}(\text{viph})_2$  reagent in a reaction with  $\text{CuCl}$ , and not  $\text{CuBr}$ . We thus suggest that an important issue is to avoid bromide anions, since they show a strong propensity toward copper complexation, as seen in compounds **3** and **4**. It must be noted that despite the fact that the solution from which **4** was crystallized contained equimolar amounts of bromide and chloride, only bromide was found to coordinate to copper, while chloride ligands were found in the magnesium cation. When the bromide ions are eliminated completely, by treatment of **1** with dioxane, and  $\text{CuCl}$  used as the copper source, the reaction runs smoothly as indicated in Scheme 1. The yield of **6** has been found to increase if a mixture of THF and dioxane is used as solvent (e.g., route A as described in the experimental section). However, the best yield

(15) Jarvis, J. A. J.; Kilbourn, B. T.; Pearce, R.; Lappert, M. J. *Chem. Soc., Dalton Trans.* **1977**, 999.

(16) Greiser, T.; Weiss, E. *Chem. Ber.* **1976**, 109, 3142.

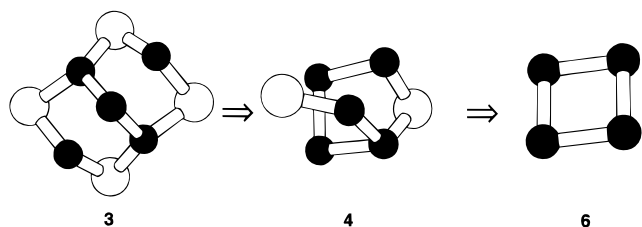


**Figure 10.** Formation of  $[\text{Cu}_4(\text{viph})_4]$  (**6**) from  $[\text{Cu}_5(\text{viph})_2\text{Br}_4]^-$  (**3**) and  $[\text{Cu}_5(\text{viph})_4\text{Br}_2]^-$  (**4**) according to stoichiometry. Only  $\text{Cu}\cdots\text{Cu}$  contacts shorter than 2.5 Å are indicated.

was obtained in route B when **2** and CuCl were reacted in toluene, although this required a somewhat longer reaction time. In route C, it was tested if exclusion of THF and inclusion of bromide anions would be a feasible synthetic strategy, since—just as using CuCl and **2**—this would eliminate any risk of precipitation of **3** or **4**. Indeed, route C, which thus involves reaction of a (viph)-MgBr diethyl ether complex with CuBr in toluene, gave **6** in acceptable yield, but the product was slightly discolored. In view of these convenient preparative routes, we believe that  $\text{Cu}_4(\text{viph})_4$  may prove to have important precursor qualities for the preparation of new copper(I) complexes. However, although mesitylcopper, which is a frequently used precursor, suffers from some drawbacks (such as ease of oxidation,<sup>17</sup> slow solid state–solution equilibrium,<sup>18</sup> and reduced reactivity on account of steric hindrance) it probably still is the best choice for the majority of situations, especially when taking the availability of 2-bromostyrene, as compared to 2-bromomesitylene, into consideration. On the other hand, 2-chlorostyrene is less expensive than 2-bromostyrene and could provide a viable alternative for larger scale synthesis of  $[\text{Cu}_4(\text{viph})_4]$ .

It is tempting, on strictly stoichiometric grounds, to suggest that complexes **2**, **3**, **4**, and **6** lie, in that order, along a straight reaction coordinate axis as indicated in Figure 10, but it must be taken into consideration that complex **3** can only be crystallized after the addition of dioxane and that the reactions in solution are governed by a complicated set of equilibria. Either way, it should be noted that the anion in compound **4** is a mere dissociation of  $\text{CuBr}_2^-$  away from the homoleptic tetramer **6** and thus provides mechanistic information concerning arylcopper formation reactions. From Figures 3, 5, 8, and 10 it is clear that, besides the obvious fact that the bromide content is gradually lowered and the vinylphenyl content is gradually raised in the formation of **6** via **3** and **4**, also the number of  $\pi$ -coordinated viph ligands forms a series that decreases (2, 1, 0) as **6** is formed. Finally, Figure 10 indicates the similarity between the cuprate in **3** and the presumed dimeric structure of many *in situ*  $\text{LiR}_2\text{Cu}$  reagents as well as crystallographically determined solid state structures like  $[\text{Li}_2\text{Ph}_4\text{Cu}_2(\text{Et}_2\text{O})_2]$ .<sup>19</sup>

The infrared spectrum of a THF solution of **6** shows only one strong absorption at  $1625\text{ cm}^{-1}$ , indicating that  $\pi$ -coordination does not occur in solution, as was ob-

served in the solid state structure of **6**. Consistent with these solution IR data are the  $^1\text{H}$  NMR data from THF solution. Although the vinyl proton resonances show some splitting, this should rather be accounted for by variable positions of the *ipso*-carbons, *e.g.*, with respect to the plane formed by the four copper atoms in **6**, than interaction of the double bond with copper. Alternatively, as cryoscopic investigations of related arylcopper compounds in benzene seem to suggest,<sup>18</sup> the cooccurrence of dimeric species would offer an explanation to the splitting pattern. Neither **3** nor **4** could be investigated with NMR due to limited solubility and, above all, the high tendency of such solutions/suspensions to decompose. Infrared solid state data for compound **3**—absorption bands at 1566, 1550, and  $1526\text{ cm}^{-1}$ —support the indication from the  $\pi$ -coordinated C=C bond lengths in the crystal structure, which suggests that these interactions are weak. The assignment of copper-coordinated C=C double bond vibrations in the infrared spectra of **3** is, however, difficult on account of interfering C–C vibrations in the  $1500\text{--}1600\text{ cm}^{-1}$  range.

Mixed halide/arylcopper complexes were previously known for aryl ligands with nitrogen donor substituents, and van Koten *et al.* have suggested that they may, in some cases, be regarded as assemblies of halocuprates (or neutral halocopper species) and arylcopper species.<sup>1,7d</sup> This is a description that could account for both  $[\text{Cu}_5(\text{viph})_2\text{Br}_4]$  and  $[\text{Cu}_5(\text{viph})_4\text{Br}_2]$ , the former being comprised of  $[\text{CuBr}]_4$  and  $[\text{Cu}(\text{viph})_2]^-$ , or alternatively of two  $[\text{CuBr}_2]^-$  anions and one  $[\text{Cu}_3(\text{viph})_2]^+$  cation, and the latter being comprised of  $[\text{CuBr}_2]^-$  and  $[\text{Cu}_4(\text{viph})_4]$ . It is reported that many of the mixed halide/arylcopper complexes with nitrogen donor substituents are quite stable, and further elimination of halide leading to homoleptic copper compounds is not possible.<sup>1</sup> In contrast, we find that **3** and **4**, which are only stabilized by  $\pi$ -coordination, are very reactive and must be described as sensitive intermediates, a circumstance that is further underlined by the unusual coordination geometries exhibited by the copper clusters. Also, all attempts to prepare **3** or **4** from **6** by adding CuBr and  $\text{MgCl}_2$  in THF were unsuccessful, yielding only decomposing solutions.

In conclusion, we have found that bromide-bridged species often precipitate from THF solutions of (viph)-MgBr and copper halides, thus preventing a clean synthesis of homoleptic (vinylphenyl)copper (**6**). The best synthetic route to **6** therefore seems to involve reacting bromide-free  $\text{Mg}(\text{viph})_2$  with CuCl in either THF or toluene. Homoleptic (vinylphenyl)copper has interesting precursor qualities and further stresses the fact that the tetrameric square-planar structure is central in organocopper chemistry.

## Experimental Section

**Synthesis. General Details.** All operations were carried out under nitrogen or argon using special low-temperature methodology<sup>20</sup> or standard Schlenk techniques (centrifugation under argon was preferred to filtration). Solvents (dioxane, hexane, tetrahydrofuran, diethyl ether, toluene) were distilled under nitrogen from sodium/benzophenone shortly prior to use. Copper(I) chloride and copper(I) bromide were purified according to literature methods.<sup>1b,21</sup> Triphenylphosphine was

(17) Håkansson, M.; Örtendahl, M.; Jagner, S.; Sigalas, M.; Eisenstein, O. *Inorg. Chem.* **1993**, *32*, 2018.

(18) Meyer, E. M.; Gambarotta, S.; Floriani, C.; Chiesi-Villa, A.; Guastini, C. *Organometallics* **1989**, *8*, 1067.

(19) Lorenzen, N. P.; Weiss, E. *Angew. Chem., Int. Ed. Engl.* **1990**, *29*, 300.

(20) Håkansson, M. *Inorg. Synth.*, in press.

(21) Keller, R. N.; Wyckoff, H. D. *Inorg. Synth.* **1946**, *2*, 1.

recrystallized from hot ethanol. Commercial 2-bromostyrene was used without further purification.

**Preparation of (viph)MgBr (1) in THF.** To a slight excess of magnesium (0.16 g, 6.6 mmol) in 20 mL of THF was 2-bromostyrene (1.10 g, 6.0 mmol) added slowly. The reaction started immediately, and the solution was cooled. The solution was left to react under stirring during 12 h, in order to ensure that all 2-bromostyrene had reacted. The solution was centrifuged, and the brownish solution was withdrawn with a syringe for further syntheses. In our experience, it is easier to handle a THF solution of **1** than the solid reagent. Evaporation under reduced pressure of the THF solution of **1** yielded a white solid that is sparingly soluble in toluene. All attempts to grow X-ray quality crystals of **1** were unsuccessful.

**Preparation of [Mg(THF)<sub>2</sub>(viph)<sub>2</sub>] (2).** To 20 mL of a 0.30 M solution of (viph)MgBr in THF was added 6 mL dioxane, and the resulting solution was stirred for 1 h. The precipitate was removed by centrifugation and the solution evaporated under reduced pressure to dryness. In order to remove dioxane completely, THF (2 × 5 mL) was added and the solution was evaporated to dryness. Yield: 1.05 g, 90%. <sup>1</sup>H NMR (THF-*d*<sub>8</sub>, 20 °C): δ 5.23 (d, 1H, =CH<sub>2</sub>), 5.46 (d, 1H, =CH<sub>2</sub>), 6.88 (t, 1H, C<sub>6</sub>H<sub>4</sub>), 6.91 (t, 1H, C<sub>6</sub>H<sub>4</sub>), 6.93 (dd, 1H, -CH=), 7.36 (d, 1H, C<sub>6</sub>H<sub>4</sub>), 7.64 (d, 1H, C<sub>6</sub>H<sub>4</sub>). X-ray quality crystals of **2** were grown from a 1:5 THF/diethyl ether solution at -80 °C.

**Preparation of [Mg(THF)<sub>6</sub>][Cu<sub>5</sub>(viph)<sub>2</sub>Br<sub>4</sub>]<sub>2</sub>·THF (3).** Purified CuCl (0.66 g, 6.7 mmol) was added to 20 mL of a 0.30 M THF solution of **1** at -30 °C. While the reaction solution slowly warmed up, CuCl dissolved, yielding a yellow solution that gradually darkens. At 10 °C the solution was brown, and a white precipitate had formed. When dioxane (5 mL) was added, the white precipitate dissolved yielding a green solution, and a gray precipitate formed. The green solution was separated by centrifugation, and yellow crystals of **3** precipitated in approximately 50% yield at 4 °C. Crystals of **3** are sparingly soluble in THF, yielding unstable solutions. The remainder of the green solution was evaporated to dryness under reduced pressure and extracted with toluene to give **6** in low yield (<5%).

**Preparation of [Mg(THF)<sub>5</sub>Cl][Cu<sub>5</sub>(viph)<sub>4</sub>Br<sub>2</sub>]<sub>2</sub>·THF (4).** Purified CuCl (0.48 g, 4.8 mmol) was added to 15 mL of a 0.30 M THF solution of **1** at -20 °C. While the reaction solution was slowly warmed to -10 °C, CuCl dissolved, yielding a yellow solution. When the solution was kept at -20 °C for several weeks, yellow crystals of **4** formed in approximately 40% yield. Crystals of **4** are sparingly soluble in THF, yielding unstable solutions.

**Preparation of [Cu(PPh<sub>3</sub>)<sub>3</sub>Br]·THF (5).** To a solution of triphenylphosphine (0.58 g, 2.21 mmol) in 5 mL of THF were added crystals of **3** (0.20 g, 0.09 mmol). After complete dissolution by gentle heating, the solution was left at ambient temperature. Colorless crystals of **5** formed after a few days. Yield: 0.05 g, 55%.

**Preparation of [Cu<sub>4</sub>(viph)<sub>4</sub>] (6). Route A: From [Mg(THF)<sub>2</sub>(viph)<sub>2</sub>] (2) and CuCl in THF.** A solution of **2** (0.40 g, 1.07 mmol) in 3 mL of THF was slowly added to a suspension of CuCl (0.22 g, 2.22 mmol) in 10 mL of THF and 3 mL of dioxane, at 0 °C. The solution was kept at 0 °C, under stirring, for 7 h. The green suspension was centrifuged and the solution evaporated to dryness under reduced pressure. In order to remove dioxane completely, THF (2 × 5 mL) was added, and the solution was evaporated to dryness. The remainder was extracted with toluene and the solution separated by centrifugation and evaporated under reduced pressure to dryness. The remaining white powder was washed with cold hexane (3 × 5 mL) and dried under argon. Yield: 0.24 g, 65%. <sup>1</sup>H NMR (THF-*d*<sub>8</sub>, 50 °C): δ 5.23 (d, 1H, =CH<sub>2</sub>), 5.92 (d, 1H, =CH<sub>2</sub>), 7.00 (t, 1H, C<sub>6</sub>H<sub>4</sub>), 7.19 (t, 1H, C<sub>6</sub>H<sub>4</sub>), 7.24 (dd, 1H, -CH=), 7.37 (d, 1H, C<sub>6</sub>H<sub>4</sub>), 7.92 (d, 1H, C<sub>6</sub>H<sub>4</sub>). Solid **6** is air-sensitive but can be stored under argon at ambient temperature without extensive decomposition. Solutions of

pure **6** in THF or toluene are remarkably stable, compared to the instability of solutions containing **3** or **4**. X-ray quality crystals of **6** were grown from a toluene solution at -80 °C.

**Route B: From [Mg(THF)<sub>2</sub>(viph)<sub>2</sub>] (2) and CuCl in Toluene.** To a solution of **2** (1.31 g, 3.49 mmol) in 50 mL of toluene was added CuCl (0.82 g, 8.28 mmol) at 0 °C. The solution was kept at ambient temperature, under stirring, for 12 h. The resulting suspension was centrifuged and the solution evaporated to dryness under reduced pressure. The residue was washed with three 5-mL portions of hexane and dissolved in the minimum amount of THF at ambient temperature. A white solid (**6**) was precipitated from this THF solution by the addition of 25 mL of hexane and dried under vacuum. Yield: 0.85 g, 73%.

**Route C: From (viph)MgBr/Ether and CuBr in Toluene.** A 0.30 M (20 mL) THF solution of **1** was evaporated to dryness under reduced pressure and washed with 10 mL of hexane. The remaining solid was dissolved in 5 mL of diethyl ether and evaporated to dryness under reduced pressure; this procedure was repeated once. The remaining solid was dissolved in 50 mL of toluene, and 1.72 g of CuBr (120 mmol) was added at 0 °C. The solution turned yellow, and a white precipitate was formed. After approximately 70 min a yellow precipitate started to form, and the green reaction solution was evaporated to dryness. The remainder was washed by sonication with 10 mL of hexane, and the solid remainder was treated with 10 mL of THF. To the resulting greenish solution was added 50 mL of hexane, yielding a light-green powder (**6**). Yield: 0.60 g, 30%.

**NMR Spectroscopy.** All NMR spectra were recorded on a Varian XL 400 spectrometer with a measuring frequency of 400 MHz <sup>1</sup>H in THF-*d*<sub>8</sub>.

**IR Spectroscopy.** Infrared spectra were collected, from -100 °C to ambient temperature, with a Mattson Polaris FTIR spectrometer, using a CaF<sub>2</sub> mull cell with pentane as mulling agent or a solution cell with CaF<sub>2</sub> windows, at a resolution of 2 cm<sup>-1</sup> and 10–100 scans.

**X-ray Crystallography. General Details.** Crystal and experimental data are summarized in Table 1. Crystals were isolated, selected, and mounted, by the use of special low-temperature methodology,<sup>20</sup> under argon, at -150 °C, and transferred (in Lindemann capillaries) under liquid nitrogen to a Rigaku AFC6R diffractometer. Diffracted intensities were measured using graphite-monochromated Mo Kα (λ = 0.710 69 Å) radiation from a RU200 rotating anode source operated at 9 kW (50 kV; 180 mA). The ω/2θ scan mode was employed, and stationary background counts were recorded on each side of the reflection, the ratio of peak counting time vs background counting time being 2:1. Data were measured for 5 < 2θ < 50°, using an ω scan rate of 8–16°/min and a scan width of (1.10 + 0.30 tanθ)°. Weak reflections (I < 10.0σ(I)) were rescanned up to three times and counts accumulated to improve counting statistics. The intensities of three reflections monitored regularly after measurement of 150 reflections confirmed crystal stability during data collection. Correction was made for Lorentz and polarization effects. No correction was made for the effects of absorption, owing to the inability to measure and index the faces of the unstable crystals and a failure to obtain a more satisfactory structural models from empirically corrected data (by means of azimuthal scans with transmission factors in the 0.90–1.00 range). However, care was taken to select and cut the crystals so that the effects of absorption were minimized. Cell constants were obtained by least-squares refinement from the setting angles of 20 reflections in the range 15 < 2θ < 30°.

The structures were solved by direct methods (MITHRIL),<sup>22</sup> and the hydrogens were located from difference maps or introduced in calculated positions. All calculations were



carried out with the TEXSAN<sup>23</sup> program package. Atomic scattering factors and anomalous dispersion correction factors were taken from ref 24. Structural illustrations have been drawn with ORTEP.<sup>25</sup>

**[Mg(THF)<sub>2</sub>(viph)<sub>2</sub>] (2).** Data were measured for a crystal with dimensions 0.30 × 0.30 × 0.30 mm. Full-matrix least-squares refinement, including anisotropic thermal parameters for the magnesium and oxygen atoms and isotropic thermal parameters for the carbon atoms, and with the hydrogen atoms as a fixed contribution, gave a final  $R = 0.071$  ( $R_w = 0.074$ ) for 124 parameters and 847 observed reflections. Reflections were weighted according to  $w = [\sigma^2(F_o)]^{-1}$ . The maximum and minimum values in the final difference map were 0.33 and  $-0.24 \text{ e}^-/\text{\AA}^3$ , respectively. Final positional parameters are listed in the Supporting Information and selected interatomic distances and angles in Table 2. The crystallographic numbering is shown in Figure 2.

**[Mg(THF)<sub>6</sub>][Cu<sub>5</sub>(viph)<sub>2</sub>Br<sub>4</sub>]<sub>2</sub>·THF (3).** Data were measured for a crystal with dimensions 0.20 × 0.15 × 0.15 mm. Two disordered THF molecules with 0.5 atom site occupancy are associated with each formula unit. The hydrogen atom bonded to C(2) could not be located from difference maps and was not introduced in a calculated position. Full-matrix least-squares refinement, including anisotropic thermal parameters for the magnesium, copper, bromide, and oxygen atoms and isotropic thermal parameters for the carbon atoms, and with the hydrogen atoms as a fixed contribution, gave a final  $R = 0.062$  ( $R_w = 0.079$ ) for 267 parameters and 1797 observed reflections. Reflections were weighted according to  $w = [\sigma^2(F_o)]^{-1}$ . The maximum and minimum values in the final difference map were 1.41 and  $-0.86 \text{ e}^-/\text{\AA}^3$ , respectively. Final positional parameters are listed in the Supporting Information, and selected interatomic distances and angles are listed in Table 3. The crystallographic numbering is shown in Figures 3 and 4.

**[Mg(THF)<sub>5</sub>Cl][Cu<sub>5</sub>(viph)<sub>4</sub>Br<sub>2</sub>]<sub>2</sub>·THF (4).** Data were measured for a crystal with dimensions 0.20 × 0.20 × 0.20 mm. Two disordered THF molecules with 0.5 atom site occupancy are associated with each formula unit. One of the these THF molecules is disordered around a center of symmetry, and consequently, only the oxygen and two carbons could be located. One of the hydrogen atoms bonded to C(32) could not be located from difference maps and was not included in a calculated position. Full-matrix least-squares refinement, including anisotropic thermal parameters for the magnesium, copper, bromide, chloride, and oxygen atoms and isotropic thermal parameters for the carbon atoms, and with the

hydrogen atoms as a fixed contribution, gave a final  $R = 0.069$  ( $R_w = 0.083$ ) for 372 parameters and 2940 observed reflections. Reflections were weighted according to  $w = [\sigma^2(F_o)]^{-1}$ . The maximum and minimum values in the final difference map were 0.90 and  $-0.54 \text{ e}^-/\text{\AA}^3$ , respectively. Final positional parameters are listed in the Supporting Information, and selected interatomic distances and angles are listed in Table 4. The crystallographic numbering is shown in Figures 5 and 6.

**[Cu(PPh<sub>3</sub>)<sub>3</sub>Br]·THF (5).** Data were measured for a crystal with dimensions 0.20 × 0.20 × 0.20 mm. Full-matrix least-squares refinement, including anisotropic thermal parameters for the copper and phosphorus atoms and isotropic thermal parameters for the carbon and oxygen atoms, and with the hydrogen atoms as a fixed contribution, gave a final  $R = 0.058$  ( $R_w = 0.059$ ) for 282 parameters and 3025 observed reflections. Reflections were weighted according to  $w = [\sigma^2(F_o)]^{-1}$ . The maximum and minimum values in the final difference map were 0.65 and  $-0.46 \text{ e}^-/\text{\AA}^3$ , respectively. Final positional parameters are listed in the Supporting Information, and selected interatomic distances and angles are listed in Table 5. The crystallographic numbering is shown in Figure 7.

**[Cu<sub>4</sub>(viph)<sub>4</sub>] (6).** Data were measured for a crystal with dimensions 0.20 × 0.15 × 0.15 mm. The viph ligands are disordered, and a detailed description of the disorder is included in the Supporting Information. The disorder is chemically sound (*cf.* the displacement of the  $C_{ipso}$  carbons in (2,4,6-triisopropylphenyl)copper),<sup>9</sup> and although there are some indications of higher symmetry from cell and positional parameters, we believe that **6** is best described as triclinic, which is supported by the fact that several datasets from different crystals all gave the same result. Full-matrix least-squares refinement, including anisotropic thermal parameters for the copper atoms and isotropic thermal parameters for the carbon atoms, and with the hydrogen atoms as a fixed contribution, gave a final  $R = 0.054$  ( $R_w = 0.065$ ) for 119 parameters and 1215 observed reflections. Reflections were weighted according to  $w = [\sigma^2(F_o)]^{-1}$ . The maximum and minimum values in the final difference map were 0.88 and  $-0.52 \text{ e}^-/\text{\AA}^3$ , respectively. Final positional parameters are listed in the Supporting Information, and selected interatomic distances and angles are listed in Table 6. The crystallographic numbering is shown in Figure 8.

**Acknowledgment.** This work has been supported by a grant from the Swedish Natural Science Research Council (NFR).

**Supporting Information Available:** Tables giving complete positional and thermal parameters, as well as full geometric data on compounds **2–6** (115 pages). Ordering information is given on any current masthead page.

OM960477C

(23) TEXSAN-TEXRAY Structure Analysis Package; Molecular Structure Corp., The Woodlands, TX, 1989.

(24) *International Tables for X-Ray Crystallography*; Kynoch Press: Birmingham, England, 1974; Vol. IV.

(25) Johnson, C. K. ORTEP. Report ORNL-3794; Oak Ridge National Laboratory, Oak Ridge, TN, 1965.